Proceedings of the SPIE's Conference on Smart Structures and Materials, Passive Damping and Isolation, Vol 3327
pp. 19-26 (1998)

Dissipative properties of granular ensembles

C. Salueña[a], S. E. Esipov[b], T. Pöschel[c] and S. Simonian[d]

[a]Departament de Física Fonamental, Divisió de Ciències Experimentals i Matemàtiques,
Universitat de Barcelona, Spain
[b]P. O. Box, New York, NY 10005
[c]Humboldt-Universität zu Berlin, Institut für Physik, Invalidenstraße 110,
D-10115 Berlin, Germany
[d] TRW Space & Electronics Group, One Space Park
Redondo Beach, CA 90278

ABSTRACT

We investigate collective dissipative properties of vibrated granular materials by means of molecular dynamics simulations. The rate of energy loss indicates three different phases in the amplitude-frequency plane of the external forcing, namely solid, convective and gas-like regimes. The behavior of the effective damping decrement is consistent with the glassy nature of granular solids. The gas-like regime is most promising for practical applications.

Keywords: Damping regimes, Molecular Dynamics simulations.

The present study of energy dissipation in granular systems is motivated by the practical interest in damping properties of granular materials.[1–3] The dominating approach in the world of vibration control and suppression has been mainly practical, given that the importance of these damping materials is widely recognized. Granular motion relaxes rapidly once the energy source of motion is suppressed; so that granular fillings, by means of internal motion, can easily absorb energy released by a shock or produced by stationary external forcing.

As we will show, granular systems reveal a number of damping regimes for different parameters A and ω of the vibrations, which are poorly understood as far as the theory of *collective* damping is concerned. The dissipation properties of dense granular systems may depend on many parameters involved, i.e. frequency and amplitude of vibration, size, roughness and hardness of particles, filling factor, size and shape of the apparatus and initial conditions.[4–6] In this article we want to restrict our investigation to study the reaction of the system to the choice of parameters of shaking A and ω, keeping all other parameters fixed.

The system we want to investigate is sketched in Fig. 1. A container which is partially filled with granular material is shaken horizontally. According to the dissipative character of the material in the box, the motion has to be driven by an external oscillator $x(t) = A\sin(\omega t)$. The system is simulated in two dimensions using molecular dynamics technique and the value of interest is the rate of dissipated energy.

In all simulations presented here, we use 500 circular particles with radii homogeneously distributed in $[0.6, 1.4]cm$ and density $2\,g/cm^2$, placed in a square container of side $L = 100\,cm$. The filling fraction is 20%. The rough inner walls of the container are simulated by attaching additional particles of the same material properties (this simulation technique is similar to "real" experiments, e.g.[7]). In the numerical experiments, the quantity measured is the mean cycle-averaged dissipation in the box under stationary conditions of oscillatory motion.

Further author information:
C.S (correspondence): Email: clara@hermes.ffn.ub.es; Telephone: 34-3-4021150; Fax: 34-3-4021149; T.P: Email:thorsten@sp10.physik.hu-berlin.de; Telephone:49-(0)30-2093-7896; Fax: 49-(0)30-2093-7638.

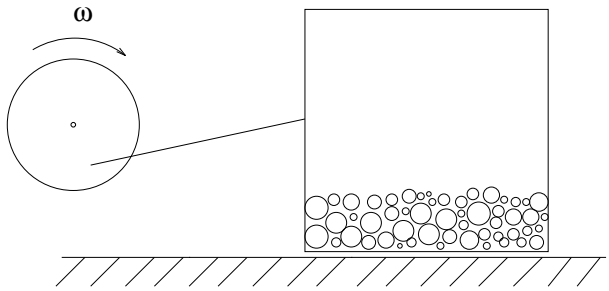

Figure 1. Scheme of the simulated system.

For the molecular dynamics simulations, we have to specify the force acting between colliding particles. We use a modified soft-particle model by Cundall and Strack[8]: Two particles i and j, with radii R_i and R_j and at positions $\vec{r}_i$ and $\vec{r}_j$, interact if their overlap $\xi_{ij} = R_i + R_j - |\vec{r}_i - \vec{r}_j|$ is positive. In this case the colliding spheres feel the force

$$\vec{F}_{ij} = F_{ij}^N \cdot \vec{n}^N + F_{ij}^S \cdot \vec{n}^S \tag{1}$$

with $\vec{n}^N$ and $\vec{n}^S$ being the unit vectors in normal and shear direction. The normal force acting between colliding spheres reads

$$F_{ij}^N = \left(Y \sqrt{R_{ij}^{\mathit{eff}}} \right) / \left(1 - \nu^2 \right) \quad \left(\frac{2}{3} \xi^{3/2} + A \sqrt{\xi}\, \dot{\xi} \right) \tag{2}$$

where Y is the Young modulus, ν is the Poisson ratio and A is a material constant which characterizes the dissipative character of the material. $R_{ij}^{\mathit{eff}} = (R_i \cdot R_j) / (R_i + R_j)$ is the effective radius of the spheres i and j. For a strict derivation of (2) see.[9–11]

For the shear force we apply the model by Haff and Werner[12]

$$F_{ij}^S = \mathrm{sign}\left(v_{ij}^{\mathit{rel}} \right) \min \left\{ \gamma_S m_{ij}^{\mathit{eff}} \left| v_{ij}^{\mathit{rel}} \right| \ , \ \mu \left| F_{ij}^N \right| \right\} \tag{3}$$

with the effective mass $m_{ij}^{\mathit{eff}} = (m_i \cdot m_j) / (m_i + m_j)$ and the relative velocity at the point of contact

$$v_{ij}^{\mathit{rel}} = \left(\dot{\vec{r}}_i - \dot{\vec{r}}_j \right) \cdot \vec{n}^S + R_i \cdot \Omega_i + R_j \cdot \Omega_j \ . \tag{4}$$

Ω_i and Ω_j are the angular velocities of the particles.

The resulting momenta M_i and M_j acting upon the particles are $M_i = F_{ij}^S \cdot R_i$ and $M_j = -F_{ij}^S \cdot R_j$. Eq. (3) takes into account that the particles slide upon each other for the case that the Coulomb condition $\mu \cdot \mid F_{ij}^N \mid \ < \ \left| F_{ij}^S \right|$ holds, otherwise they feel some viscous friction. By means of $\gamma_n \equiv AY/(1-\nu^2)$ and γ_S, normal and shear friction coefficients, dissipation during particle contact is taken into account.

The values of the coefficients used in simulations are $Y/(1-\nu^2) = 7.5 \times 10^7$, $\gamma_n = 7 \times 10^2$, $\gamma_S = 30$, $\mu = 0.5$, all in cgs units.

With the system parameters specified above, depending on forcing one observes intensive convection (Fig 2). The existence of convection patterns in horizontally vibrated granular material has been reported recently.[13–15] In our case only two rolls could be observed. Different aspect ratios or material parameters may give different convection patterns, with 2, 4[13] or more convection rolls.

The velocity profiles in Fig. 2 have been produced by averaging particle velocities over 30 cycles, after the system reached a steady state regime. We do not want to discuss the effect of convection in horizontally shaken material in detail, but we only want to show that the onset of convection in the system is due to a critical amplitude of driving velocity $[A\omega]_{cr}$, since this is crucial for the further discussion.

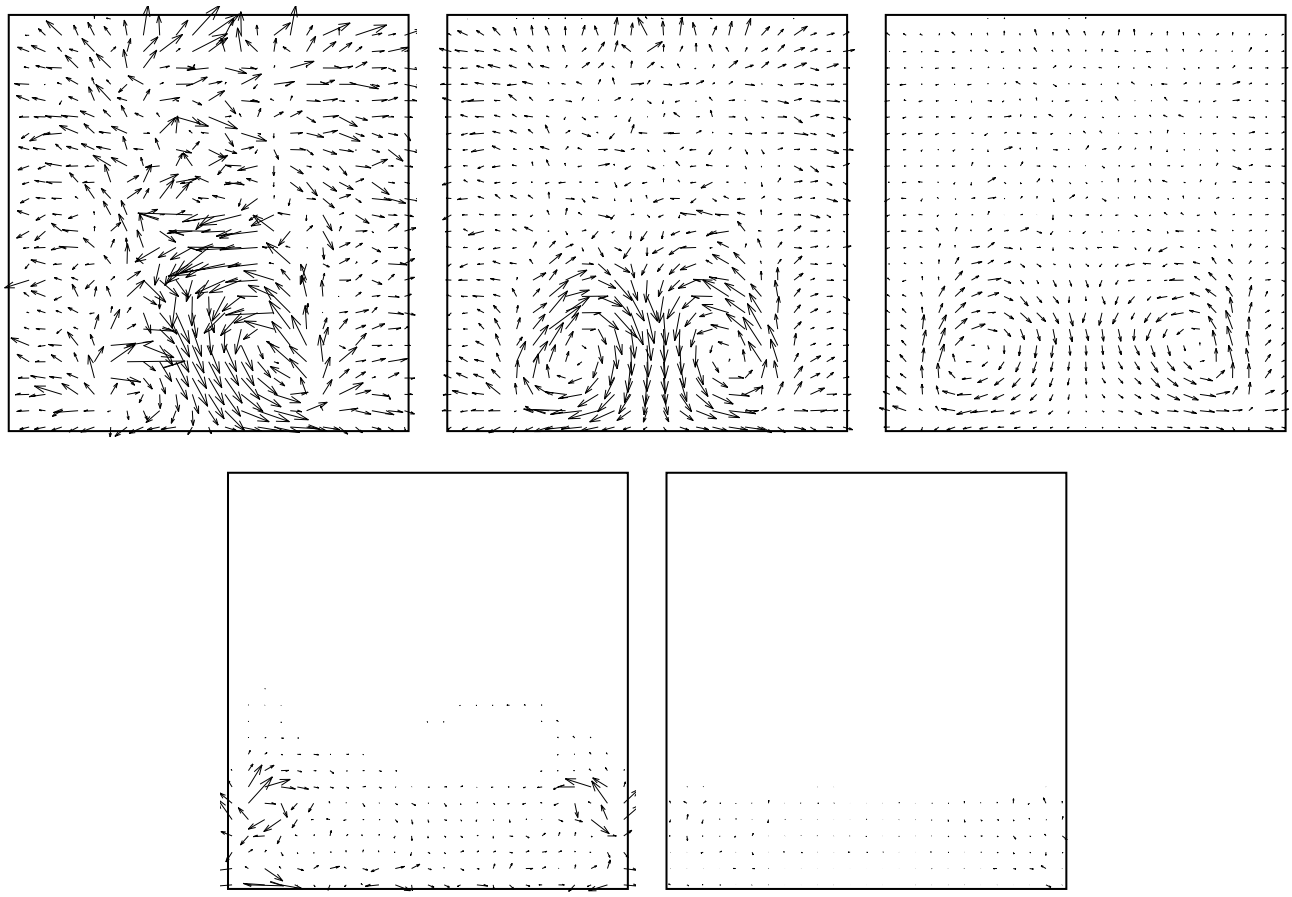

Figure 2. Images of the cycle-averaged motion of the system vibrated at $f = 20$ for different velocities of forcing, $A\omega$: a) 1900, b) 1250, c) 600, d) 100, e) 15.

Fig. 3 shows the maximum absolute value of convective motion in the system, i.e. the length of the longest arrow in Fig. 2 over the velocity amplitude $A\omega$ for different frequencies. Below $[A\omega]_{cr} \approx 80$ there is only small collective motion in the system, but close to this point there is a relatively sharp transition into the convective regime.

To characterize the dissipation in the system we introduce an effective damping parameter

$$b = \frac{\frac{1}{T}\int_T W_{diss}(t)dt}{m\omega^2 A^2} \tag{5}$$

which is proportional to the ratio between the averaged dissipated power per cycle T and the mean translational kinetic energy of the granular system of total mass m. The rotational energy has not been taken into account in the denominator of (5) because the rotational energy represents a small fraction of the translational kinetic energy (less than 10%). Note that b is clearly a constant for a linear damped oscillator, equal to the inverse of the amplitude relaxation time.

Fig. 4 shows the damping b as a function of the forcing parameter, $\Gamma = A\omega^2/g$ (effective acceleration) and the amplitude of the velocity of vibration, $A\omega$. Different symbols (filled or open) code for different frequencies. Except for the very low frequency range, b scales with the amplitude of the velocity of vibration, $A\omega$ (Fig. 4 (top)). A transition from the $A\omega$-scaling into another regime takes place at $\Gamma \approx 1$ (Fig. 4 (bottom)). Below this point the effective damping parameter becomes less sensitive to Γ.

Fig. 4 reveals three regions, indicative of different dynamic regimes. Let us start the discussion in the "valley" of Fig. 4 (top), which is the region surrounding the local minimum. This is the region of spatially organized behavior

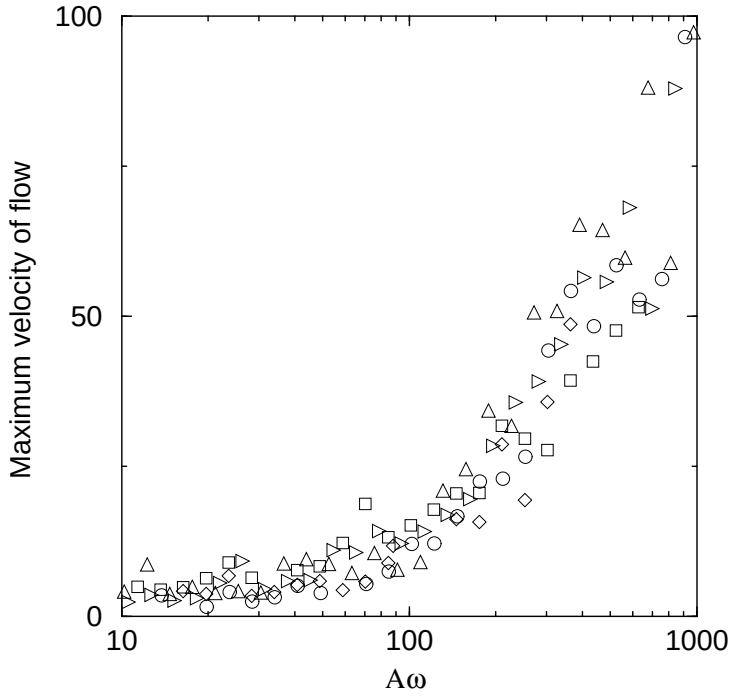

Figure 3. Maximum velocity of collective flow V over amplitude of shaking velocity $A\omega$, both in cm/s, for the different frequencies analyzed: $\diamond$: 5; $\square$: 10; $\circ$: 20; $\triangleright$: 40; $\triangle$: 80.

with well developed convection rolls, where the entire granular mass participates in collective motion (Fig. 2c). It is interesting to stress that this region corresponds to a minimum rate of energy dissipation, compared to the energy of motion.

For higher velocity amplitudes $A\omega$, dissipation increases, as particles begin to fly across the box and the ordered structure of the rolls starts to disappear (cf. Fig. 2a-b). The minimum corresponds to a characteristic velocity at which the system starts to transit into the gas state. This value can be obtained approximately by equating the characteristic time of motion in horizontal and vertical directions for a particle with velocity of the order of $A\omega$,

$$L/A\omega = A\omega/g\,. \tag{6}$$

For $L = 100$, this gives $A\omega \approx 300$, which is close to the value at the minimum of Fig. 4 (top). At this point, particles may stay airborne and gravity becomes unimportant. Thus, the boundary $A\omega = \sqrt{Lg}$ separates the "liquid" and gas-like regimes.

Preliminary experiments in the range of studied frequencies and velocities show that the observed damping parameter reproduces very well the qualitative behavior about the local minimum of Fig. 4 (top), which can be located with a good precision by using (6).

On the left side of the valley, as amplitude decreases for any frequency, the depth of the rolls diminishes progressively until a critical value $[A\omega 1]_{cr} \approx 80$ is reached. At this velocity the rolls vanish completely and we do not find organized motion in the system anymore. The critical value is represented in Fig. 4 (top) by a change in slope.

Following Fig. 4 (bottom) to yet smaller amplitudes, we find another change in behavior at about $\Gamma \approx 1$, i.e. when the maximal acceleration of shaking becomes comparable with gravity g. For $\Gamma > 1$ the curves are smooth, but for $\Gamma \sim 1$ suddenly the data become very noisy. At this point the grains condense to a solid phase, i.e. we have a solid-fluid transition as it has been studied recently by Ristow et al.[16] The fluidization point found in Ref.[16]

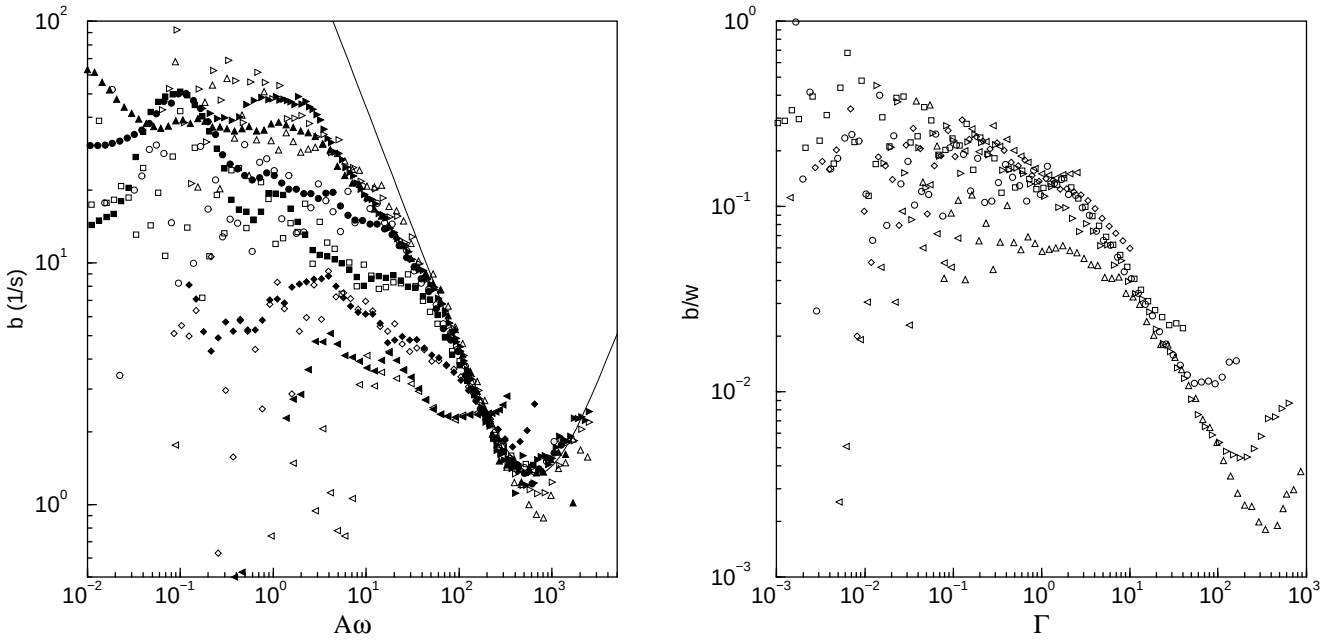

Figure 4. Effective damping parameter b vs the amplitude of velocity of vibration, $A\omega$ (top) and vs the the forcing parameter, $\Gamma = A\omega^2/g$. Different symbols refer to different frequencies; $\triangleleft$: 2.5; $\diamond$: 5; $\square$: 10; $\circ$: 20; $\triangleright$: 40; $\triangle$: 80. Open symbols refer to fast cooling schedule, filled symbols to slow cooling (see text for details). The solid line is the best fit by using both (8) and(7).

agrees completely with the value $A\omega^2 = g$ from our analysis. At the transition point the particles get trapped in their momentary position. In this solid phase the grains constitute a block which still dissipates energy, since even when no shearing exists, there is deformation energy loss (through the coefficient γ_n). Therefore, in the solid regime the rate of dissipated energy depends strongly on the configurational arrangement of the particles. This configuration depends on the history of the system, i.e. for the same parameters of oscillation A and ω, depending on initial conditions, the system can reach different configurational arrangements, which lead to different values of the dissipation rate. To demonstrate this fact, in Fig. 4 (top) we have drawn data points with filled and open symbols which refer to "fast" and "slow" cooling. By fast cooling we mean an instantaneous transition from any fluidized initial state to the specified amplitude and frequency of vibration. The initial conditions, namely, random positions and velocities of particles, are kept the same for each data point. Thus, there is no memory of the preceding evolution. Having the first 30 cycles of the driving oscillation discarded, the mean dissipation is obtained by averaging over 30 cycles of shaking in the way specified above. The large fluctuation of the dissipation rate b is not due to insufficient data averaging; averaging over 100 cycles, instead of 30, leads to the same results. In the case of slow cooling, the system is initialized only once for each frequency, and the final state for a certain amplitude A serves as the initial one for the next amplitude to be investigated. The amplitude of vibration in each simulation is diminished by a factor 1.2. The behavior in this case can be sensitive to the entire history of the system. According to the mechanism discussed in Fig. 4 (top), in the region $\Gamma \lesssim 1$ the fast cooling data points begin to fluctuate, whereas the slow cooling data are relatively smooth.

On the (A, ω) plane the regime boundaries form a diagram similar to the Van der Waals system, with the triple point $(L, \sqrt{g/L})$. Above this point, direct "sublimation" is achieved at $A\omega^2 \approx g$. Convection rolls can develop at $A < L$ above a critical velocity, as has been discussed. This diagram is shown in Fig. 5.

The fluidized regime is adequate for hydrodynamical analysis. First consider the gas state, where the dissipation is entirely dominated by collisions with the walls of the container. The pressure transmitted to the vertical wall by

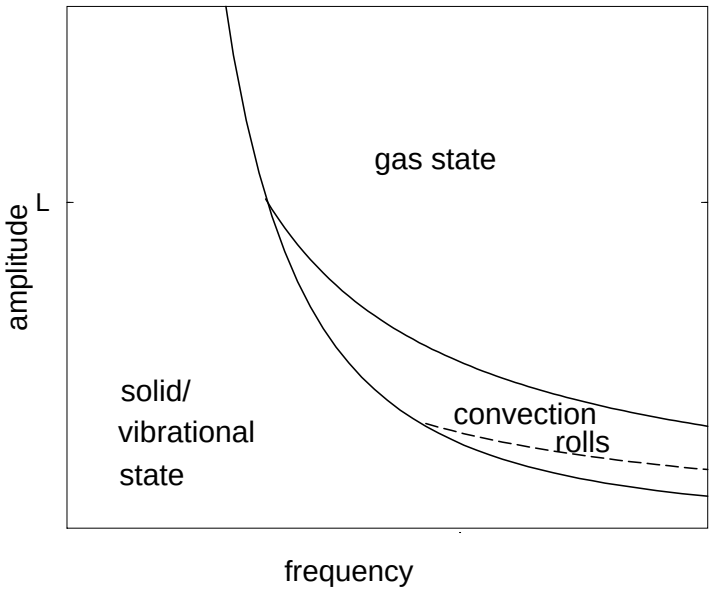

Figure 5. Phase diagram of our horizontally vibrated system, displaying the regimes found in the analysis of the damping parameter.

the granular mass of density ρ which moves with velocity $v = 2A\omega$ relative to the wall is $2\rho A^2\omega^2$. Other contributions can be neglected in this regime. Therefore, the dissipated power during the collision is then roughly a fraction of the quantity $2\rho v^3 L$. By definition (5) one finds

$$b = C_g \frac{A\omega}{L} \,. \tag{7}$$

Formula (7) is applicable at $A\omega \geq \sqrt{Lg}$ and C_g is some unknown numerical prefactor. Note that this expression is proportional to the collision frequency of gas particles moving at velocity $A\omega$ and having a mean free path of the order of L.

For velocities $A\omega < \sqrt{Lg}$, the system is only partially fluidized. This means that the pressure transmitted by the container walls does not exceed the static stresses in the material, which are roughly of the order of $p = \rho g L$ in horizontal direction. As long as there is any fluidized material in the system, these stresses cannot be lower. Therefore, the dissipated power is pHv, where H is the height of the system. Dividing it by $\frac{1}{2}\rho HLv^2$ one gets

$$b = C_l \frac{g}{A\omega} \,. \tag{8}$$

Formula (8) is applicable at $A\omega^2 \geq g$ and $A\omega \leq \sqrt{Lg}$, and C_l is the unknown numerical prefactor. The best fits for the curves of Fig. 4 provide the values $C_g = 0.1$ and $C_l = 0.45$ for our simulated system.

By means of MD simulations we have shown how the analysis of rate of energy dissipation sheds some light on collective granular dynamics. Different distinct damping regimes can be identified. Particularly, one finds that convective states correspond to local minima of rate of energy dissipation. Performing two types of measurements, referred as to slow and fast cooling, we identified a glass regime. This regime, in which configurational states affect the dynamical properties of the system, is separated from the "fluidized" regime by the value of the forcing parameter, $\Gamma \equiv Af^2/g \sim 1$. The $A\omega$-scaling of the damping curves signals the beginning of the fluid regime. Here convective states can develop in a region of the plane (ω, A) above a critical velocity and below $A = \sqrt{Lg}/\omega$. Beyond the minimum, for velocities $A\omega > \sqrt{Lg}$, a gas state can be identified, where the effects of gravity can be neglected. In this regime dissipation is the inverse time needed to cross the system with the velocity of the shaking, and the entire granular ensemble can be approximated by a single particle with translational degrees of freedom and suitable restitution coefficient. The gas regime is most promising for damping since it can maintain a super-linear positive feedback: an increase in the velocity of shaking leads to an increase in decrement.

ACKNOWLEDGEMENTS

The authors wish to thank V. Buchholtz for discussion. The calculations have been done on the parallel computer *KATJA* (http://summa.physik.hu-berlin.de/KATJA/) of the medical department *Charité* of the Humboldt University Berlin.

REFERENCES

1. C. Grubin *ASME Journal of Applied Mechanics* **23**, p. 373, 1956.
2. S. F. Masri *Journal of the Acoustical Society of America* **45**(5), p. 1111, 1969.
3. M. M. Sadek *Proceedings I. Mech. E.* **180**(1), p. 95, 1969.
4. A. Papalou and S. F. Masri *ASME Journal of Vibration and Acoustics* **118**, p. 614, 1996.
5. H. V. Panossian *ASME Journal of Vibration and Acoustics* **114**, p. 101, 1992.
6. S. S. Simonian *SPIE Proceedings* **2445**, p. 149, 1995.
7. E. E. Ehrichs, H. M. Jaeger, G. S. Karczmar, J. B. Knight, V. Y. Kuperman, and S. R. Nagel *Science* **267**, pp. 1632–1634, 1995.
8. P. A. Cundall and O. D. L. Strack *Géotechnique* **29**, p. 47, 1979.
9. G. Kuwabara and K. Kono *Jpn. J. Appl. Phys.* **26**, p. 1230, 1987.
10. N. V. Brilliantov, F. Spahn, J. M. Hertzsch, and T. Pöschel *Phys. Rev. E* **53**, p. 5382, 1996.
11. W. A. M. Morgado and I. Oppenheim *Phys. Rev. E* **55**, p. 1940, 1997.
12. P. K. Haff and B. T. Werner *Powder Technol.* **48**, p. 239, 1986.
13. K. Liffman and G. Metcalfe in *Powders and Grains '97*, R. P. Behringer and J. T. Jenkins, eds., p. 405, Balkema, (Rotterdam), 1997.
14. C. Salueña, S. E. Esipov and T. Pöschel in *Powders and Grains '97*, R. P. Behringer and J. T. Jenkins, eds., p. 341, Balkema, (Rotterdam), 1997.
15. C. Salueña, S. E. Esipov and T. Pöschel, "Hydrodynamics of dense granular systems," in *Smart Structures and Materials: Passive Damping and Isolation.*, vol. 3045 of *SPIE Proceedings*, p. 3, 1997.
16. G. H. Ristow, G. Straßburger and I. Rehberg *Phys. Rev. Lett.* **79**(5), p. 833, 1997.